

Electronic Supplementary Information

for

**Synergistic Effects of Substrate-Ligand Interaction in Metal-Organic
Complexes on the De-electronation Kinetics of a Vitamin C Fuel Cell**

Muskan Parmar,^{a,#} Sanchayita Mukhopadhyay,^{a,#} Ritwik Mondal,^{a,#} Bhojkumar Nayak,^a
Neethu Christudas Dargily,^a Harish Makri Nimbegondi Kotresh,^b Chathakudath
Prabhakaran Vinod,^c and Musthafa Ottakam Thotiyl^{a,*}

^a Department of Chemistry and Centre for Energy Science, Indian Institute of Science
Education and Research, Pune, Dr. Homi Bhabha Road, Pune 411008, India.

E-mail: musthafa@iiserpune.ac.in

^b Department of Chemistry, Acharya Institute of Technology, Soldevanahalli, Bangalore
560107, India.

^c Catalysis and Inorganic Chemistry Division, CSIR-NCL, Pune 411008, India.

These authors contributed equally.

Experimental Section:

Materials

Chemicals such as N, N-dimethylformamide (DMF) (99%), hexane (95%), isopropyl alcohol (99%), copper (II) chloride hexahydrate ($\geq 98\%$), nickel (II) chloride hexahydrate (99.99%), ammonium molybdate (99.99%), phthalimide, 4-nitro phthalimide (98%), ammonium chloride ($\geq 98\%$), toluene (99.5%), methanol (99%), ethanol (95%), sulfuric acid (96%), and nitrobenzene (99%), potassium ferricyanide, potassium dihydrogen phosphate ($>98\%$), potassium hydrogen phosphate ($>98\%$) and Pt/C (40%) were procured from Alfa Aesar. Dimethyl sulfoxide-d₆ (DMSO-d₆) (99.9 atom % D), Deuterium oxide (99.9 atom % D), Nafion solutions (5 wt %) and L-Ascorbic ($\geq 99\%$), acid was procured from Sigma-Aldrich. Ketjan black (KB) was obtained from Kuraray chemicals. Toray carbon sheet (GDL) was procured from fuel cell store in USA.

Methods

Matrix-Assisted Laser Desorption Ionization Time-of-Flight Mass Spectrometry (MALDI-TOF MS) was performed using the AB SCIEX 4800 Plus TOF/TOF instrument. The light absorption by molecules was analyzed using UV-visible spectroscopy, carried out with the Perkin Elmer Lambda 950 instrument. Fourier Transform Infrared Spectroscopy (FTIR) was conducted with the Bruker Alpha ATR-FTIR instrument to provide insights into molecular structure and functional groups. Raman Spectroscopy, employed with the LabRAM HR Horiba Jobin Yvon spectrometer, enabled the study of vibrational and rotational modes in the samples. Scanning Electron Microscopy (SEM) coupled with Energy-Dispersive X-ray Spectroscopy (EDX) was performed using the Zeiss Ultraplus-4095 instrument to visualize samples and analyze their elemental composition. Zeta potential measurements, which provide information about the surface charge, were conducted using the Zetasizer Nano ZS90 Analyzer (Malvern software). X-ray photoelectron spectroscopy (XPS) analysis utilized a Thermo Scientific K alpha+ spectrometer with a micro-focused Al K α radiation source emitting at 1486.6 eV. The spectrometer maintained a base pressure below $\sim 5 \times 10^{-9}$ mbar during data collection. A 50 eV pass energy was applied for individual core level measurements. Charge compensation was performed using an electron flood gun. Peak fitting analysis was conducted employing XPS Peak Fit software with linear-type background correction.

Synthesis Procedures

Synthesis of Copper (II)phthalocyanine (CuPc), Nickel (II)phthalocyanine (NiPc), tetraaminocopper(II)phthalocyanine (TACuPc) and tetraaminonickel(II) phthalocyanine (TANiPc) molecules

Key reagents, including copper (II) chloride hexahydrate, urea, ammonium chloride, ammonium molybdate, along with phthalimide were utilized for the synthesis of unsubstituted copper (II) phthalocyanine whereas the above reagents along with 4-nitro phthalimide in place of phthalimide were used for synthesizing tetra nitro copper (II) phthalocyanine (TNCuPc). The procedure involved grinding the chemicals and combining them in a round bottom flask with nitrobenzene. The mixture was then refluxed at 180°C for 5 hours. Following it, the product was purified thoroughly. This included washing with ethanol and water to remove excess urea, hydrolysis of residual urea with 1 M KOH and dilute HCl and rinsing with ethanol and water to eliminate acidic or alkaline impurities. The product was then dried in a vacuum oven at 80°C overnight. The final products obtained were CuPc and TNCuPc respectively. The tetra nitro copper (II) phthalocyanine (TNCuPc) was further reduced to tetra amino copper (II) phthalocyanine (TACuPc) by reducing it with sodium sulfide nonahydrate. Initially, the mixture was heated at 80°C for 2 hours followed by cooling and diluting with ice water. The precipitate obtained was isolated and washed with hot water, methanol and hexane to get TACuPc. Similar procedure was followed for the synthesis of NiPc and TANiPc respectively by replacing the metal precursor from copper (II) chloride hexahydrate to nickel (II) chloride hexahydrate.¹⁻⁴

Synthesis of CuPc and TACuPc embedded on Ketjan black (KB)

A precise amount of both CuPc and TACuPc phthalocyanines were individually mixed with Ketjan Black, a modified form of carbon black, maintaining a weight ratio of 3:7 in N, N-Dimethylformamide (DMF). After 30 minutes of sonication, the mixtures were stirred for 24 hour at room temperature (RT). The resulting mixture was centrifuged to isolate the solid, which was then sequentially washed with DMF and ethanol. Finally, the solid was air-dried overnight to get the final composite material.⁵ For the preparation of anodic electrodes we maintained a similar mole ratio of both the molecules for all the experiments. To verify this, we have collected scanning electron microscopy (SEM) image along with elemental mapping

of Cu, N, and C for pristine CuPc and the TACuPc composite. The analysis indicates a fairly uniform distribution of Cu, C, and N in both pristine CuPc and the TACuPc composites, as shown in Fig. S20a-b. Additionally, the EDX spectra in Fig. S21a-b reveal that both composites have almost a similar atomic weight percentage for copper.

Experimental Methods

To investigate how the ligand functionality assists the electrochemistry, the electrochemical analysis was carried out using a Biologic VMP-300 potentiostat. For anodic half-cell electrochemistry, the ascorbic acid electrochemical oxidation was carried out first in a single-compartment electrochemical cell containing three electrodes with glassy carbon electrode (3 mm diameter) as the working electrode, Pt disc as the counter electrode, and Ag/AgCl/KCl (3.5 M) as the reference electrode. The first step involved the preparation of an ink by subjecting the molecules to sonication, using 1 mL of dimethylformamide (DMF). Subsequently, this ink was drop casted onto a glassy carbon electrode. Cyclic voltammetry was performed in argon-saturated 0.1 M phosphate buffer (pH ~7) solution with 2 mM of ascorbic acid at a scan rate of 10 mV/s. For cathodic half-cell electrochemistry, we utilized 10 mM potassium ferricyanide solution ($K_3[Fe(CN)_6]$) in Ar saturated phosphate buffer. All the experiments were carried out at room temperature (25°C). Tafel analysis was done to delve deeper into the kinetics governing the ascorbic acid (vitamin C) reaction. This analytical method involves the utilization of the Tafel equation, which is expressed as $\eta = a + b \log(j_k)$, where η represents the overpotential, 'a' signifies the Tafel intercept or the exchange current density, 'b' denotes the Tafel slope, and ' j_k ' represents the kinetic current density.

Estimation of number of electrons and rate constant via RDE

RDE measurements were performed using a glassy carbon RDE electrode in 0.1 M phosphate buffer solution at 5 mV/s scan rate. Different rotation rates (100, 225, 400, 625, 900, 1225 and 1600 rpm) were employed to perform these measurements.

The experimental data was analyzed with the help of the Koutecky-Levich equation (K-L equation). The number of electrons (n) were calculated using equation S1

$$\frac{1}{j} = \frac{1}{j_k} + \frac{1}{j_l} \quad (S1)$$

Where j is the total current density, j_k is the kinetic current density which equals $nFCk^0$ where k^0 represents the heterogeneous rate constant with unit of cm s^{-1} and j_l is the limiting current density, equation S2

$$j_l = 0.62nFD^{2/3}\nu^{-1/6}\omega^{1/2} \quad (S2)$$

Here, n is the number of electrons, F (C mol^{-1}) is the Faraday constant, D ($\text{cm}^2 \text{s}^{-1}$) is the diffusion coefficient, ν ($\text{cm}^2 \text{s}^{-1}$) is the kinematic viscosity, C (mol cm^{-3}) is the bulk concentration and ω (rad s^{-1}) is the rotation rate.

Raman spectroscopic analysis

The molecular catalyst modifications with ascorbic acid was monitored with Raman spectroscopic analysis. The catalyst coated over FTO-glass electrodes were treated with 0.1 M ascorbic acid solution and the electrode was held open circuit potential (OCV) for nearly 500 s. The Raman spectra of these treated samples were collected in distilled water using Pro Raman L, Enwave Optronics.

UV- Visible spectroscopic analysis for pK_a measurements

UV-visible absorption spectra of TACuPc and CuPc were observed as they were titrated with acid at room temperature. Perkin Elmer Lambda 950 spectrophotometer was used with 1 cm quartz cuvettes to record the spectra consistently while adding 10 μl of HCl (0.001 M). Sets of spectra representing consecutive stages of protonation were selected for detailed analysis, by employing the Hill equation (equation S3),

$$\log \frac{A_0 - A_i}{A_f - A_0} = \log K_i + n_H \log [H^+] \quad (S3)$$

Here, K_i stands for the formation constant of the i^{th} protonated species, A_0 represents the observed absorbance of the sample, A_i stands for the absorbance of the $(i-1)^{\text{th}}$ protonated form, (where $i = 1, 2, 3, 4$ etc), and A_f is the absorbance of the i^{th} protonated form. n_H is the Hill coefficient, and $[H^+]$ denotes the acid concentration.⁶

Fuel cell construction

The vitamin C fuel cell was fabricated using the composite of CuPc and TACuPc with Ketjan Black (KB) carbon as the anodic electrocatalyst. The anode was prepared by spraying the dispersed electrocatalyst's ink (electrocatalyst: KB = 3:7) on a Toray carbon sheet maintaining a loading of 2 mg/cm². The cathode preparation was done using Ketjan black, which was spray coated on Toray carbon paper with a loading of 2 mg/cm². A pretreated Nafion 117 membrane was then placed between the anode and cathode and the membrane electrode assembly was made was kept between two graphitic plates with a serpentine flow channel (1 cm² area). Inlet and outlet flow pipes were provided for both the half-cells for the flow of electrolytes. A 1 M vitamin C solution in pH 14 and pH 7 solution were employed as the anolyte. In contrast, a 0.5 M potassium ferricyanide solution in pH 14 and pH 7 solution were used as the catholyte. The volume of electrolytes used were 30 mL for each half-cell. The rate of flow for the solution was 10 mL per minute. In the case of vitamin C – precious metal-based fuel cell, commercial Pt/C (2 mg/cm²) was used as the anode catalyst and KB carbon with a loading of 2 mg/cm² was used as cathode electrode. The electrodes possessed a geometric area of 1 cm². The operating temperature for all fuel cell experiments was maintained at 25°C.

Calibration

The calibration of ferricyanide was performed via UV-visible spectroscopy at various known concentrations of ferricyanide starting from 0.5 M till 0.05 M with an interval of 0.05 M. Subsequently, a calibration plot is constructed by measuring the absorbance (at 420 nm) against known concentrations. Using this calibration plot, the unknown quantity of ferricyanide consumed at various time intervals during fuel cell operation was estimated.

The calibration of ascorbic acid was performed via UV-visible spectroscopy at various known concentrations of ferricyanide starting from 1.0 M till 0.1 M with an interval of 0.2 M. Subsequently, a calibration plot is constructed by measuring the absorbance (at 300 nm) against known concentrations. Using this calibration plot, the unknown quantity of ascorbic acid was estimated.

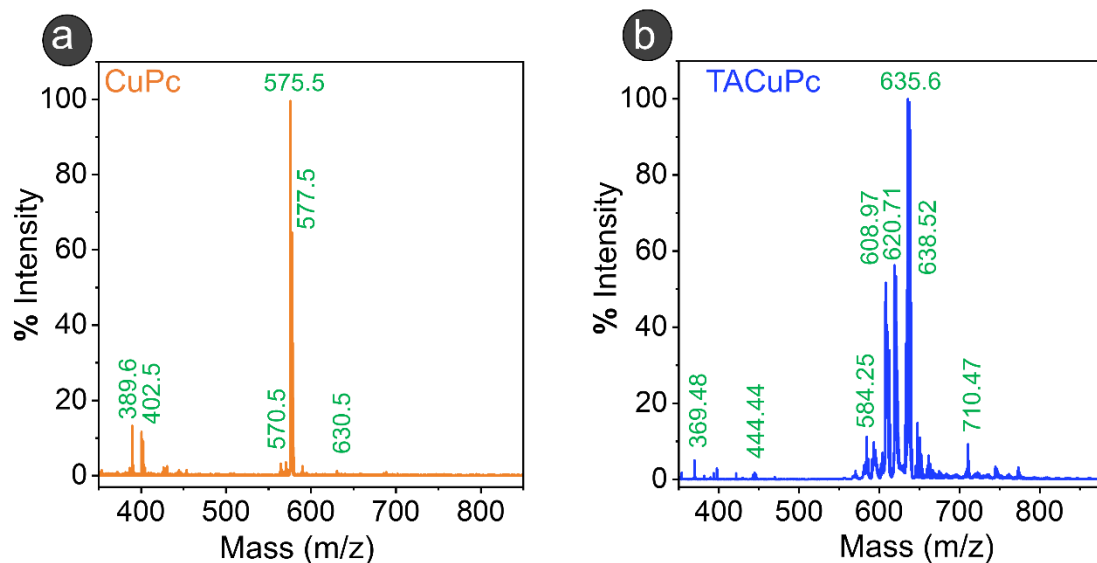


Fig. S1 Matrix assisted laser desorption ionization time of flight mass spectra (MALDI-TOF) of (a) CuPc and (b) TACuPc, respectively.

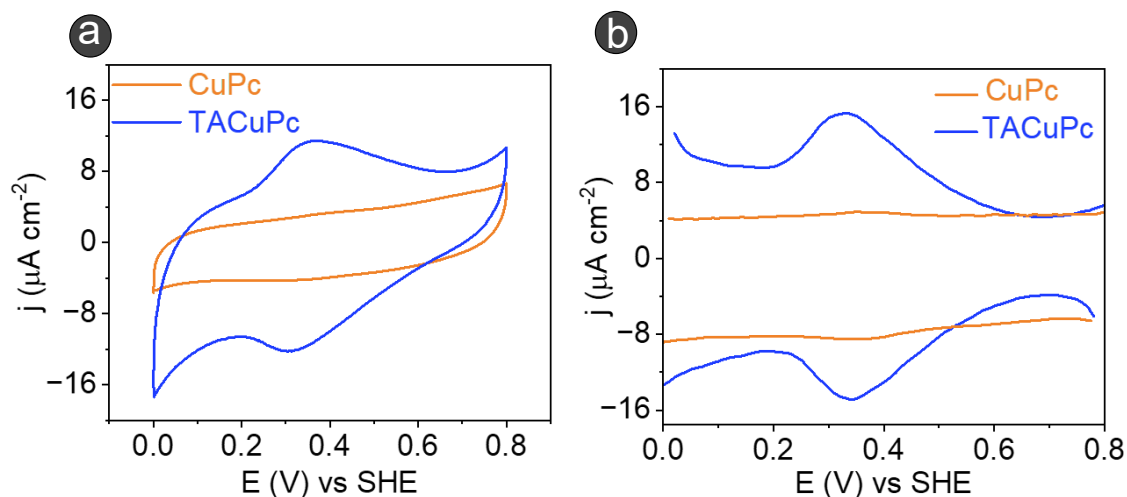


Fig. S2 a) Cyclic voltammograms and (b) differential pulse voltammograms in the phosphate buffer electrolyte (pH 7) without ascorbic acid at a scan rate of 10 mV/s.

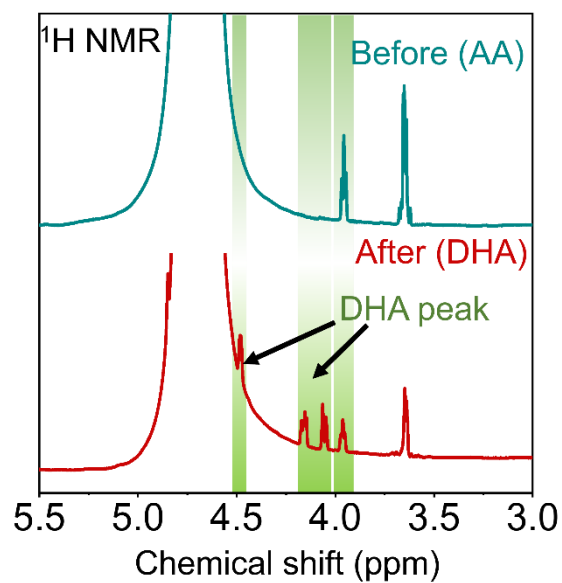


Fig. S3 ¹H NMR spectrum before reaction (AA) and after reaction (DHA) in D₂O for vitamin C oxidation.

Table S1 Comparative analysis of charge transfer resistance for TACuPc and CuPc

Parameters	CuPc	TACuPc
R _{ct} (kΩ cm ²)	12.36	5.37

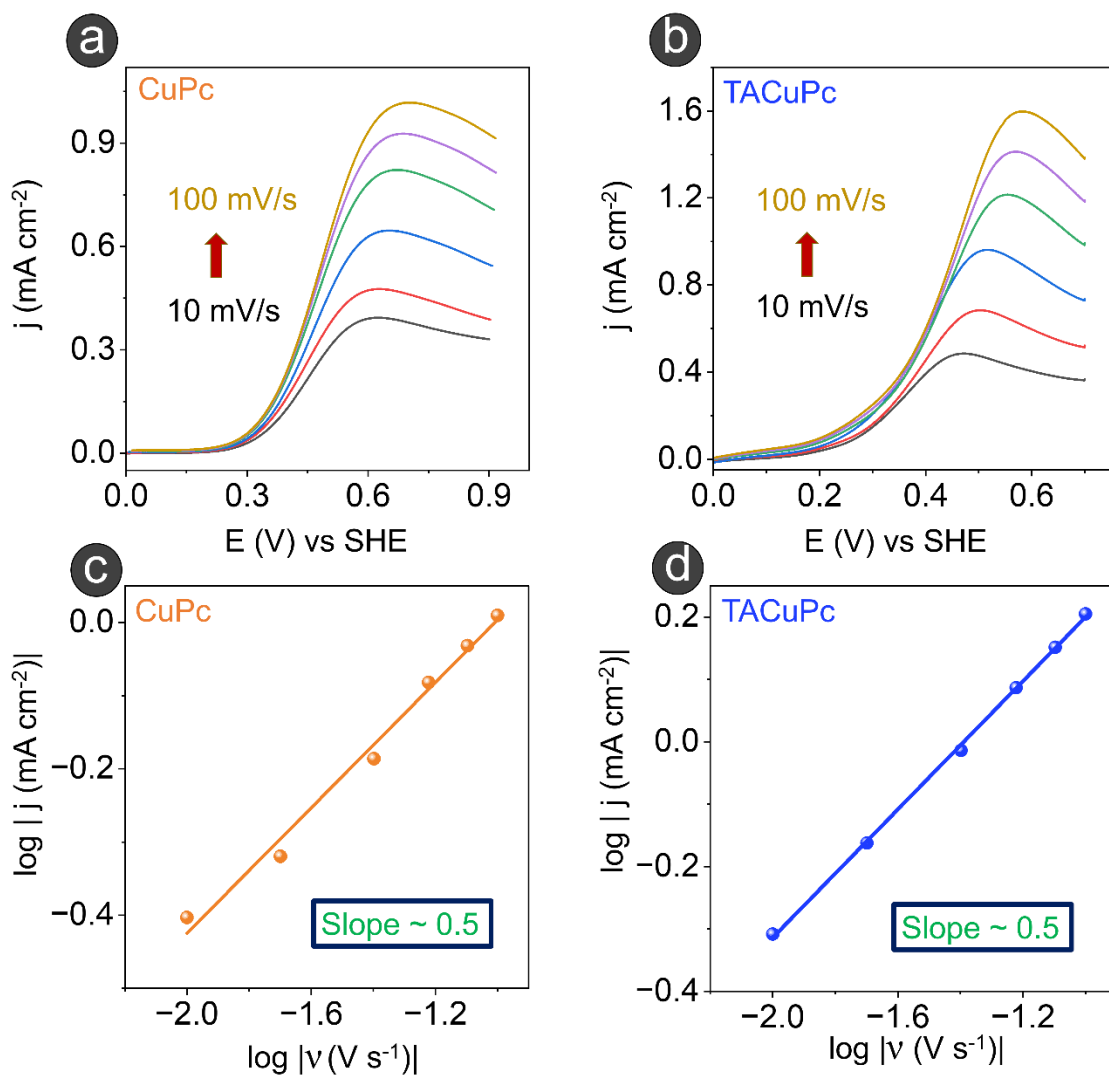


Fig. S4 (a-b) Linear sweep voltammograms illustrating the oxidation of 2 mM vitamin C in phosphate buffer (pH 7) across scan rates ranging from 10 mV/s to 100 mV/s, and (c-d) $\log j$ vs. $\log \nu$ plots corresponding to CuPc and TACuPc molecules, respectively.

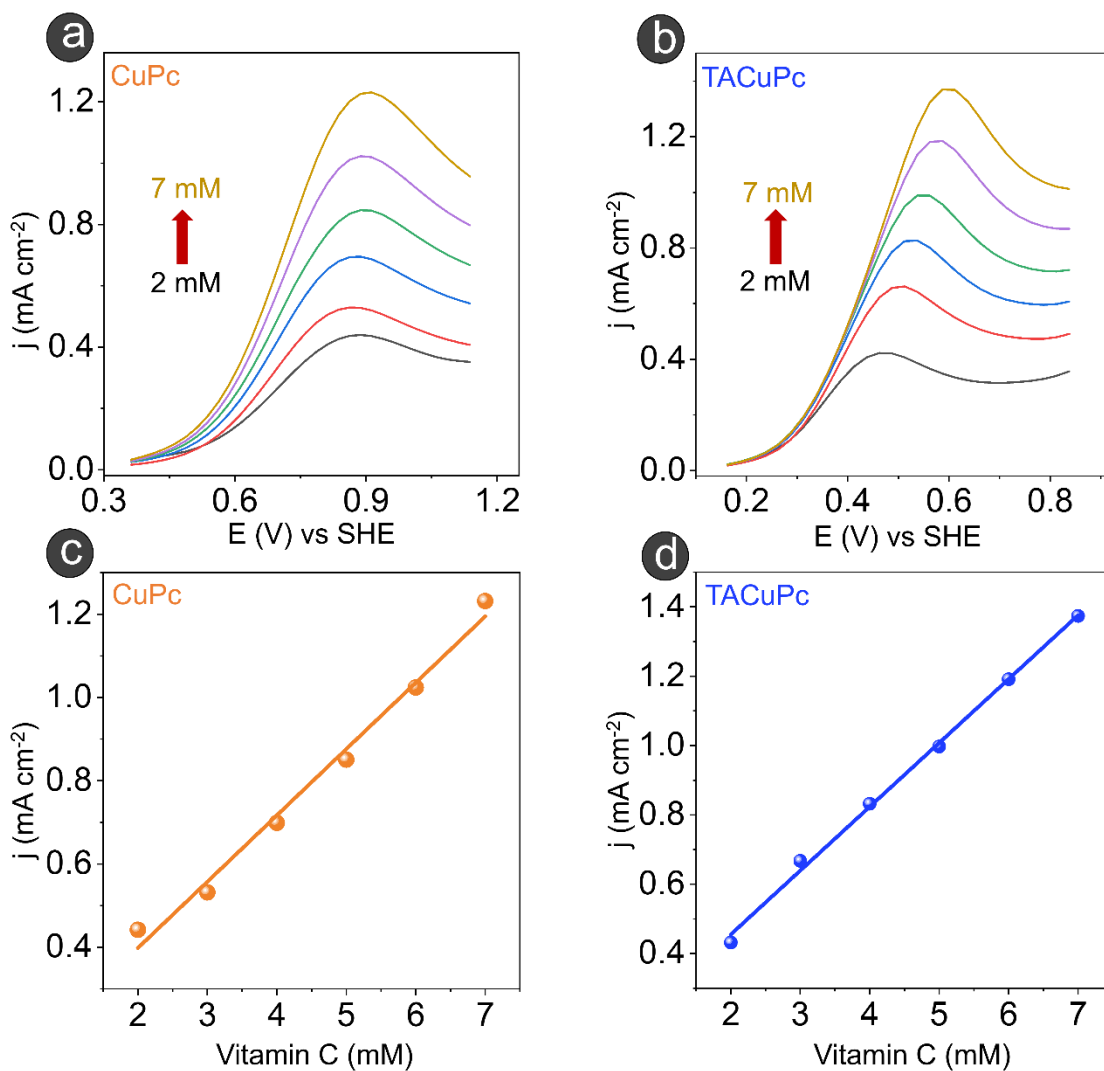


Fig. S5 (a-b) Linear sweep voltammograms depicting vitamin C oxidation in phosphate buffer (pH 7) at a scan rate of 10 mV/s, varying concentrations from 2 mM to 7 mM. (c-d) Corresponding plots of peak current versus vitamin C concentration using CuPc and TACuPc molecules, respectively.

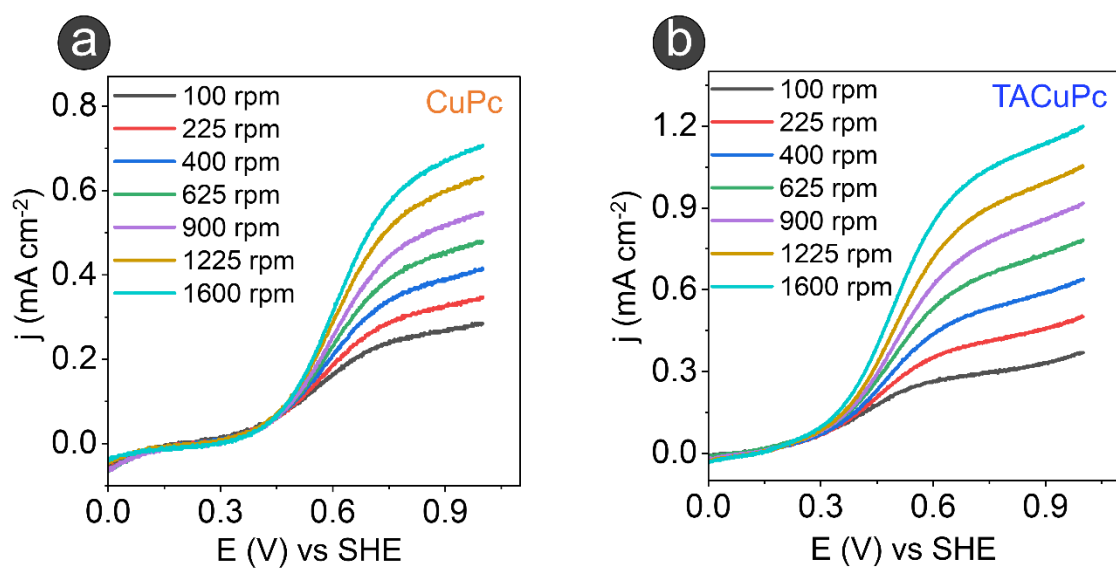


Fig. S6 Hydrodynamic study (Linear sweep voltammograms) with rotating disk electrode for vitamin C oxidation on a (a) CuPc and (b) TACuPc modified glassy carbon disk electrode in phosphate buffer of pH = 7 with different rotation rates.

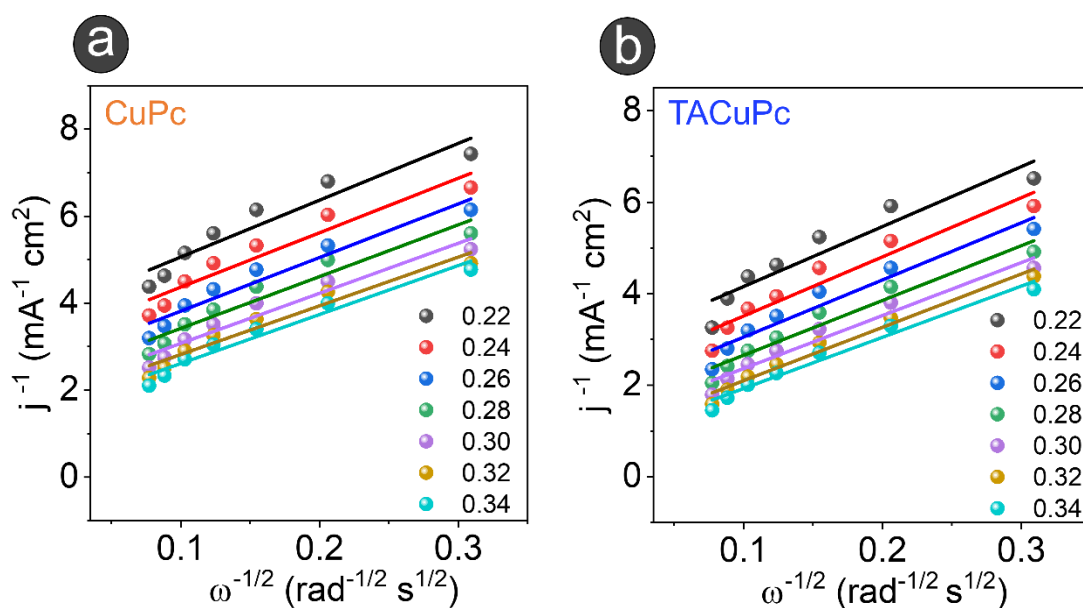


Fig. S7 Koutecky–Levich plot extracted from RDE for the oxidation of vitamin C in phosphate buffer (pH 7) at various overpotentials with respect to the onset potential of each catalyst with (a) CuPc and (b) TACuPc, respectively.

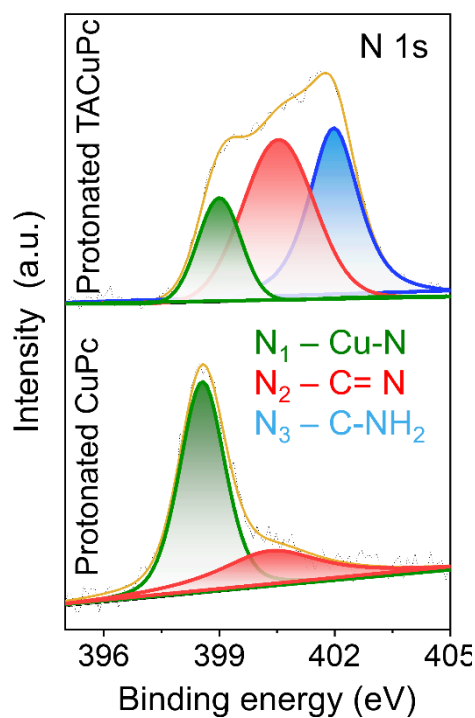


Fig. S8 N 1s XPS spectra of protonated CuPc (bottom panel) and protonated TACuPc (top panel).

Table S2 N 1s Binding energy values and the shift in binding energy (Δ BE) before and after treating CuPc and TACuPc with ascorbic acid. (N_1 : Cu-N, N_2 : -C=N, N_3 : -C-NH₂). The values are extracted from Figure 3a and 3b.

Molecules	TACuPc			CuPc	
	N_1	N_2	N_3	N_1	N_2
Pristine (eV)	398.3	399.2	400.5	398.4	399.9
Protonated (eV)	398.7	400.5	402.0	398.6	400.4
ΔBE [Protonated-Pristine] (eV)	0.4	1.3	1.5	0.2	0.5

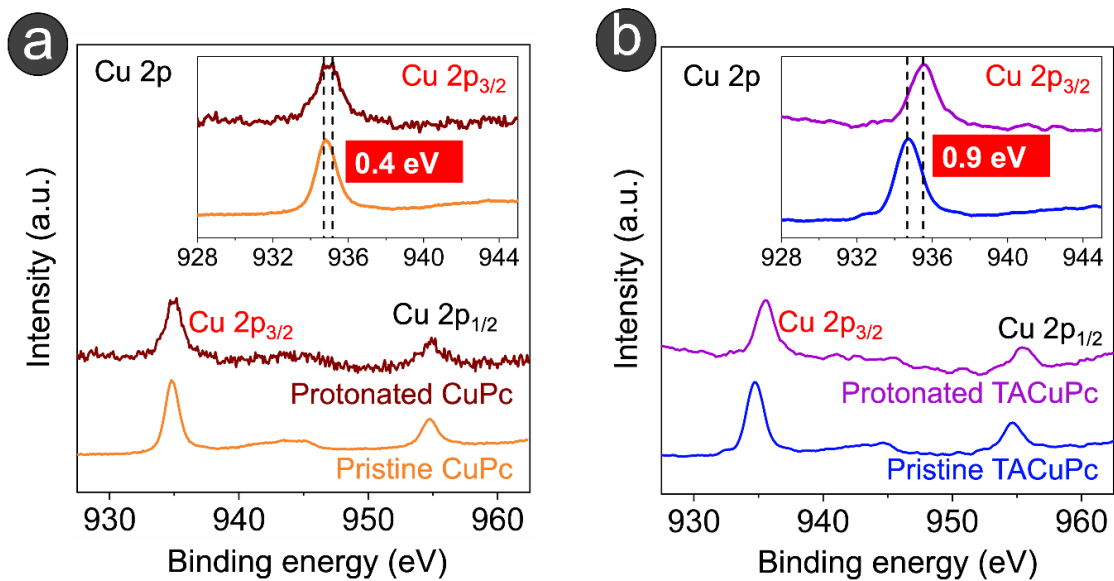


Fig. S9 Cu 2p raw XPS spectra of pristine and protonated (a) CuPc and (b) TACuPc respectively.

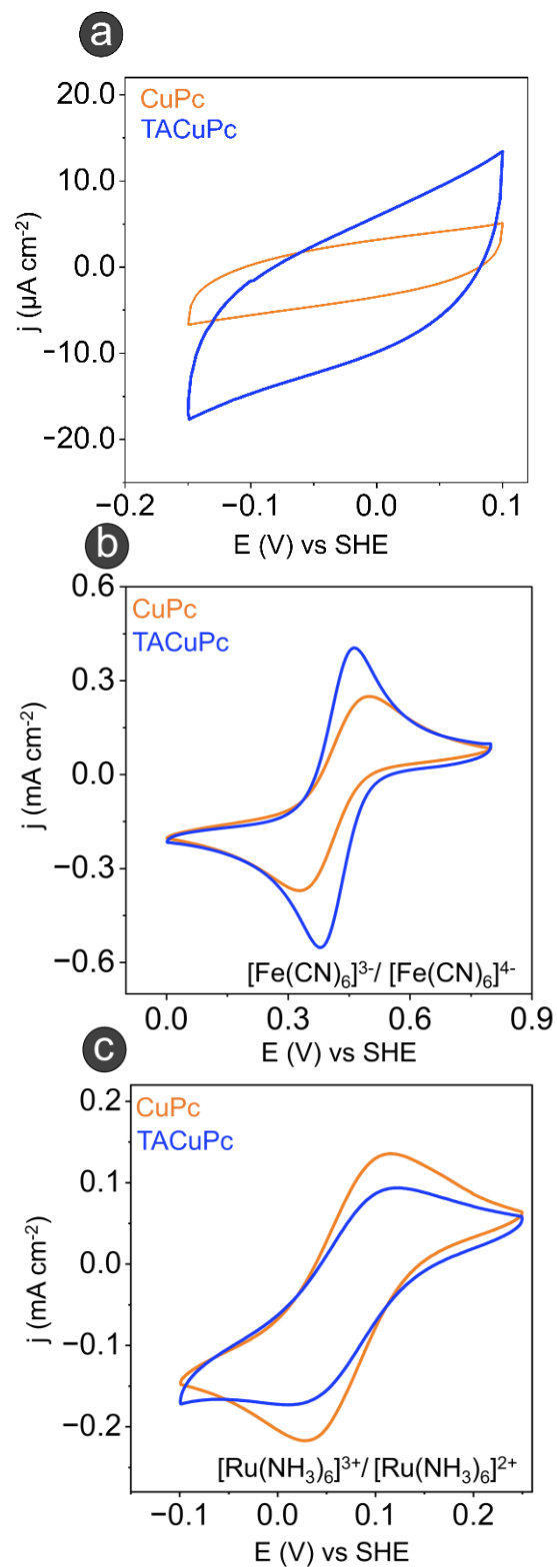


Fig. S10 (a) Electrical double layer study at a scan rate of 20 mV/s in the electrolyte solution and (b) Cyclic voltammogram at a scan rate of 20 mV/s in the presence of $[\text{Fe}(\text{CN})_6]^{3-}/[\text{Fe}(\text{CN})_6]^{4-}$ and (c) $[\text{Ru}(\text{NH}_3)_6]^{3+}/[\text{Ru}(\text{NH}_3)_6]^{2+}$ with CuPc and TACuPc in the electrolyte solution.

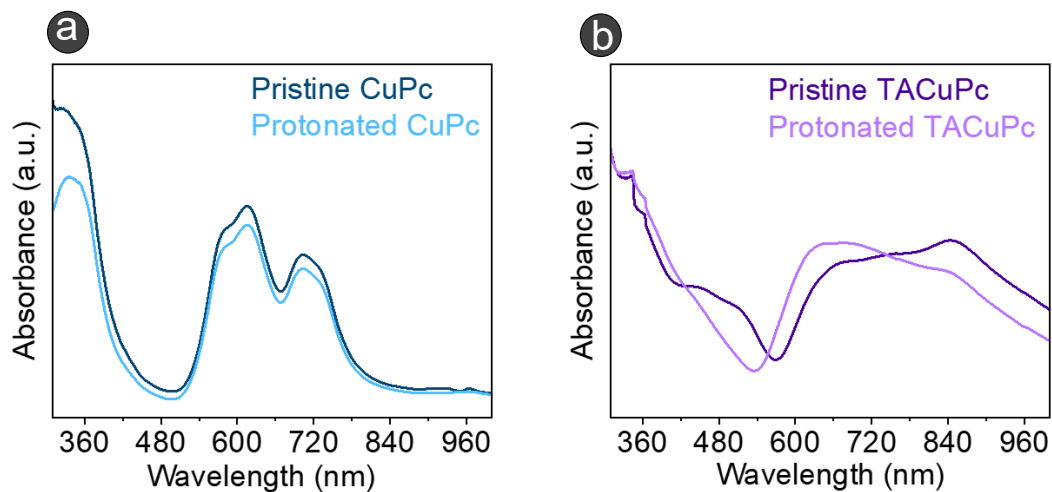


Fig. S11 UV-visible spectra of CuPc and TACuPc molecules before and after treating with ascorbic acid.

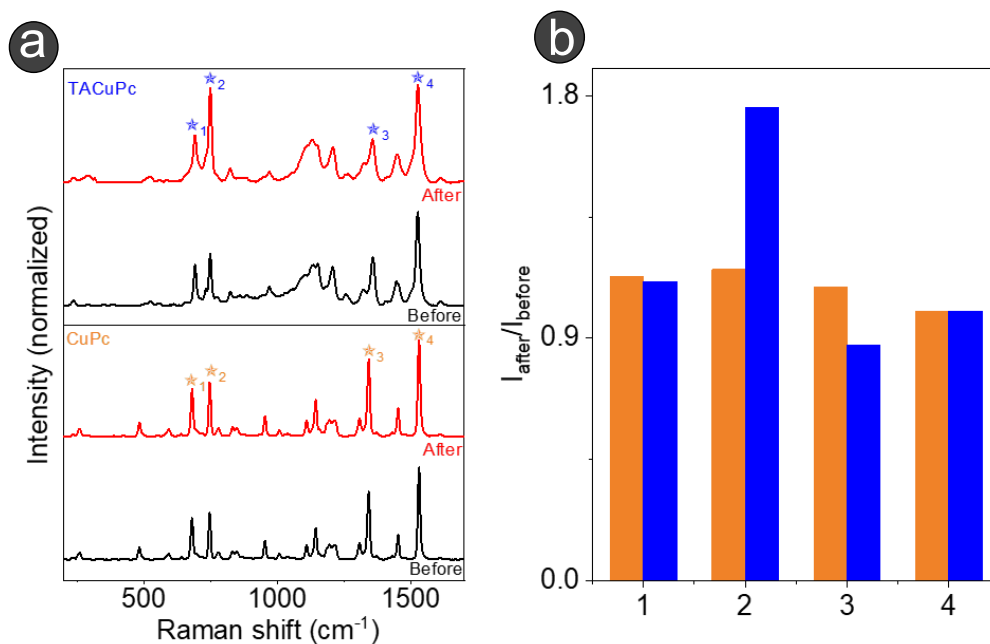
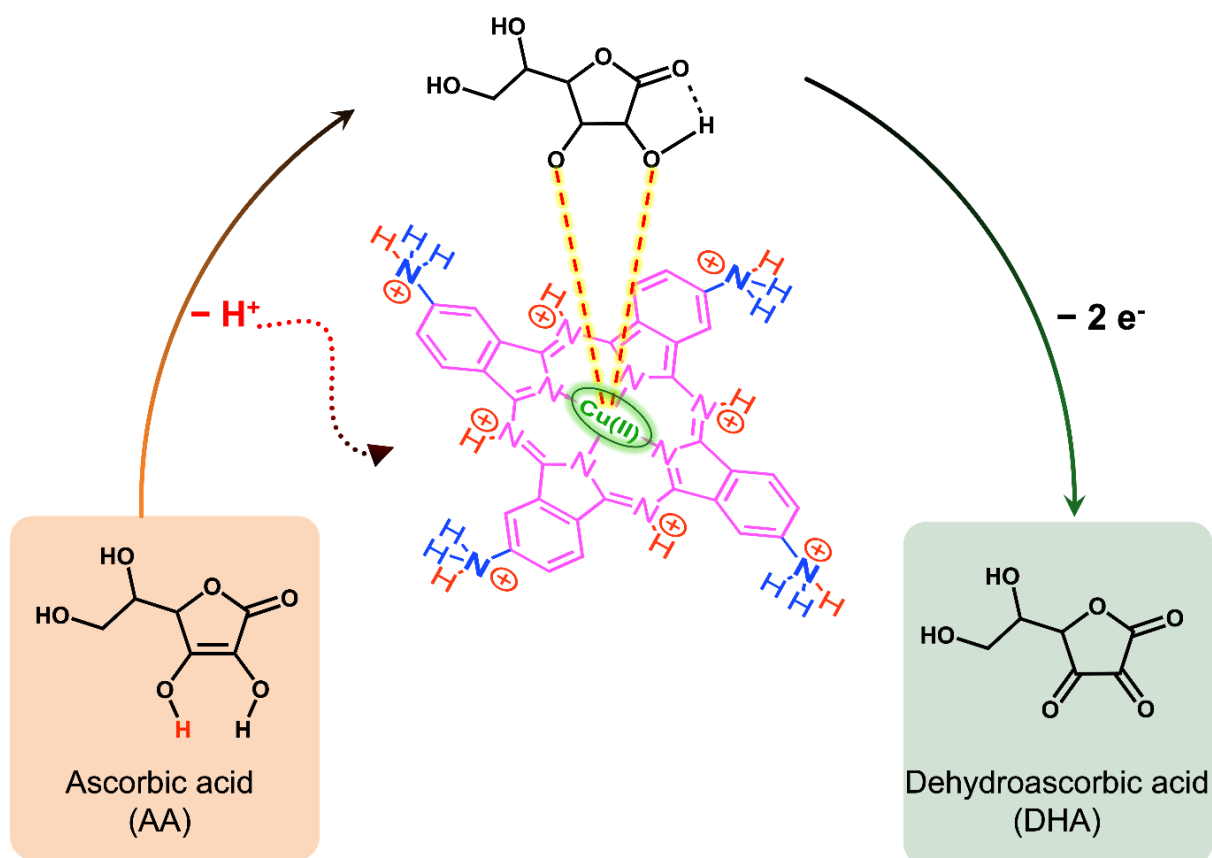


Fig. S12 (a) Raman Spectra of TACuPc (top panel) and CuPc (lower panel) before and after the addition of ascorbic acid in pH 7 solution at OCV. (b) Bar plot showing the intensity ratios after and before treating with ascorbic acid ($I_{\text{after}}/I_{\text{before}}$) for TACuPc and CuPc for the asterisk marked Raman bands (1-4).



Scheme S1. Schematic representation of mechanism of vitamin C oxidation to dehydroascorbic acid via proton charge assembly in TACuPc molecule.

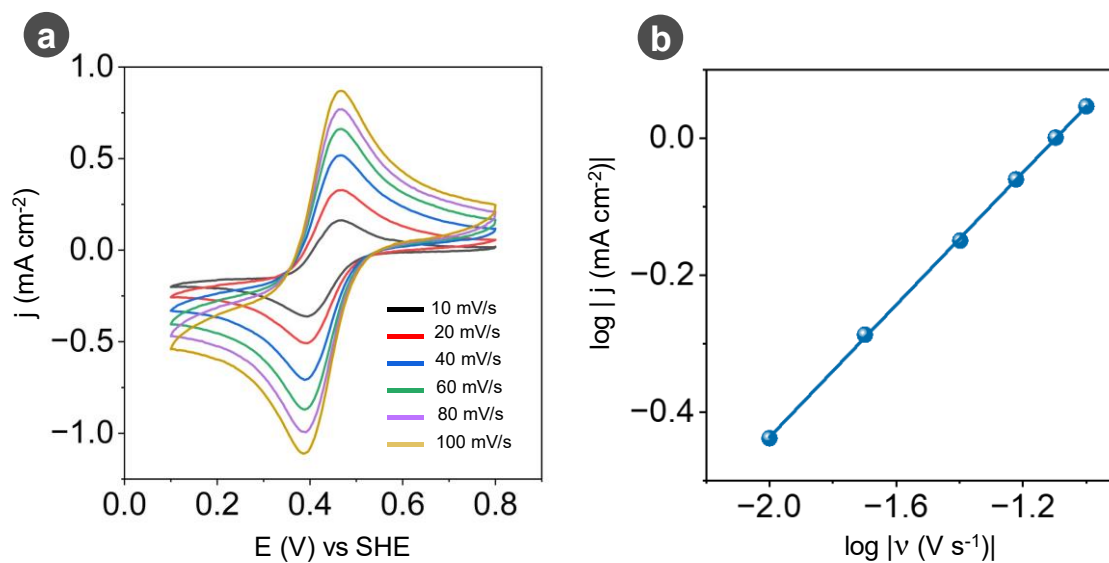


Fig. S13 (a) Cyclic Voltammogram of 10 mM potassium ferricyanide on glassy carbon electrode at different scan rates ranging from 10 mV/s to 100 mV/s in 0.1M phosphate buffer (pH 7) (b) Plot of $\log (j)$ vs. $\log v$ (Extracted from Figure. S13a).

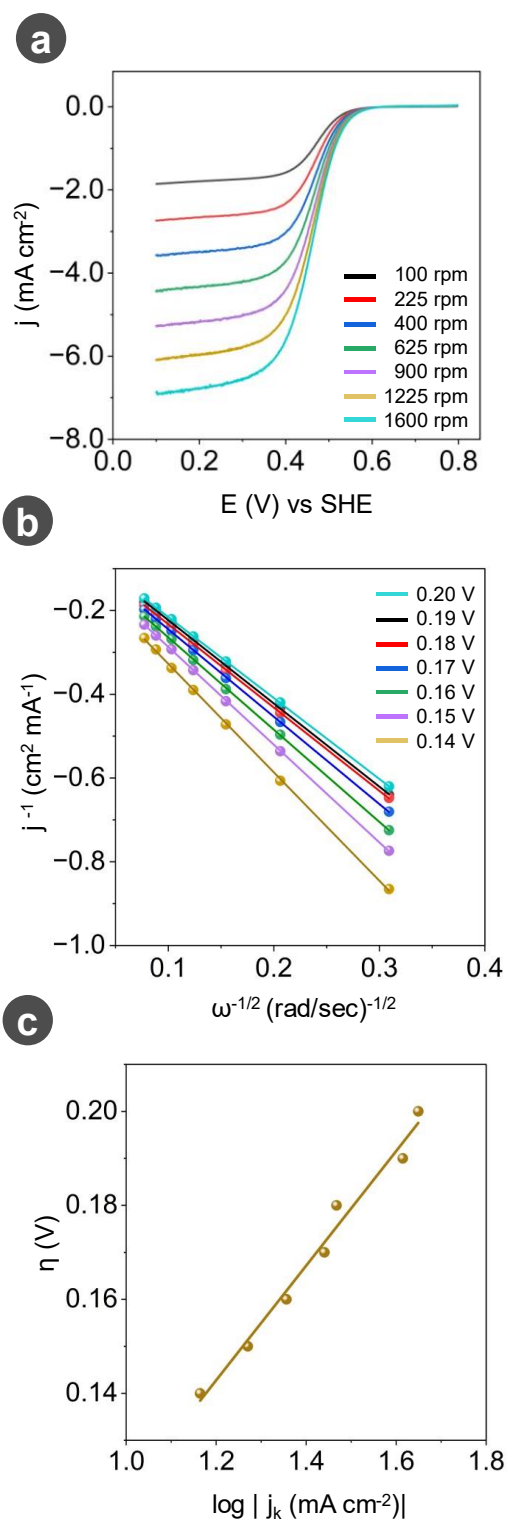


Fig. S14 (a) Hydrodynamic study (Linear sweep voltammogram) with RDE measurements for 10 mM ferricyanide on a glassy carbon disk electrode in phosphate buffer of pH = 7 with different rotation rates from 100 rpm to 1600 rpm. (b) K–L plot extracted from RDE and (c) the plot of logarithmic kinetic current density (j_k) versus overpotential (η) for the ferricyanide in phosphate buffer (pH 7) on a glassy carbon electrode.

Table S3 Comparative analysis of specific power and specific current for the TACuPc and CuPc based vitamin C fuel cells. The current and power were normalized to the actual loading of molecular catalysts in the composite electrodes. (extracted from Fig. 4b)

Molecule	Specific power density (mW mg^{-1})	Specific current density (mA mg^{-1})
CuPc	$19.8 \text{ mW mg}^{-1}_{\text{CuPc}}$	$80.7 \text{ mA mg}^{-1}_{\text{CuPc}}$
TACuPc	$24.7 \text{ mW mg}^{-1}_{\text{TACuPc}}$	$100.6 \text{ mA mg}^{-1}_{\text{TACuPc}}$

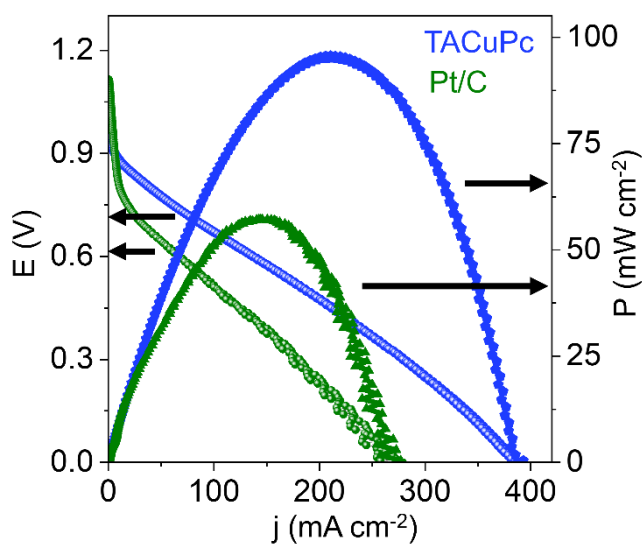


Fig. S15 Polarization curve comparing vitamin C-ferricyanide fuel cell using a carbon-based cathode with varied anodes (blue: TACuPc, green: Pt/C).

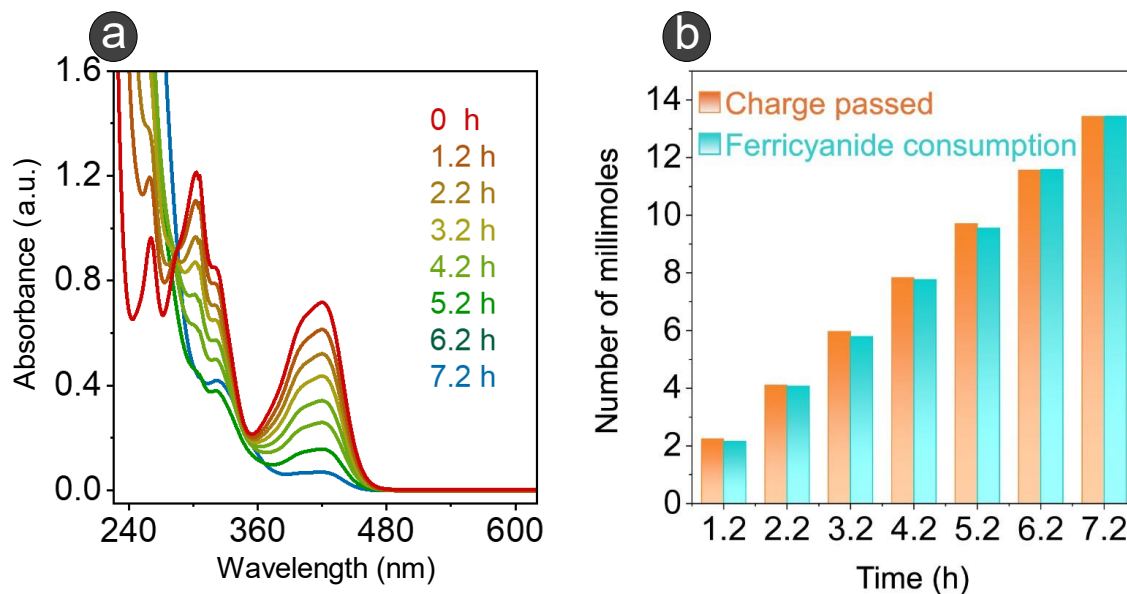


Fig. S16 (a) UV-Visible spectra of the catholyte captured at various time intervals during the chronopotentiometry measurements (corresponding to Fig. 4f). (b) Charge balance and consumption of ferricyanide during the chronopotentiometry.

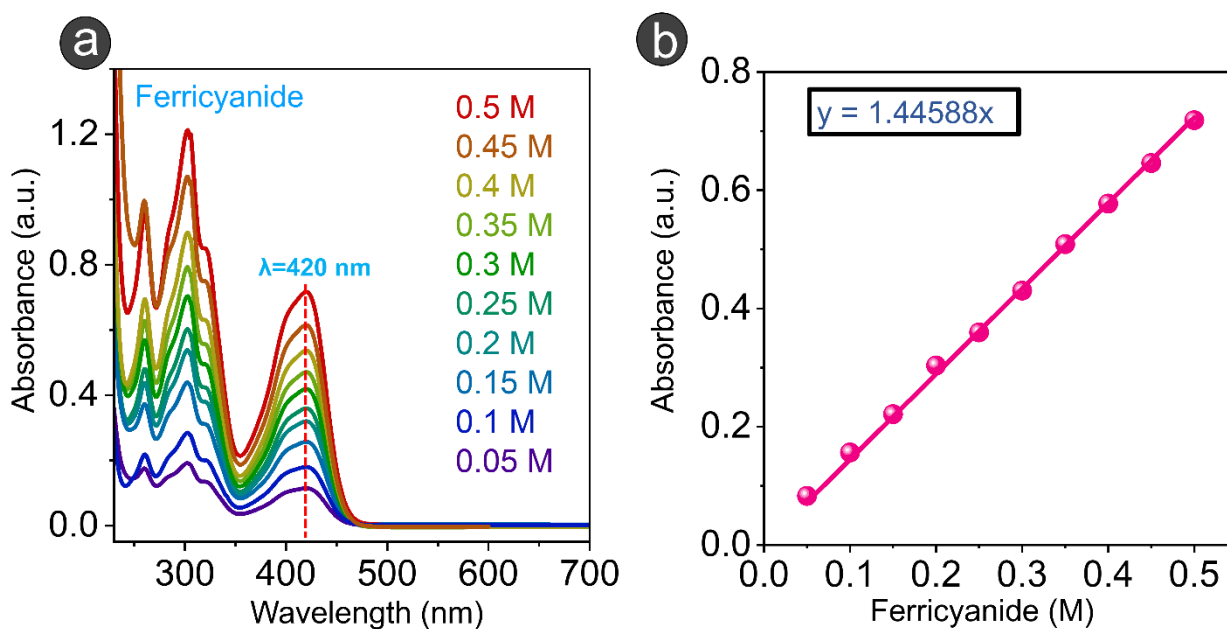


Fig. S17 (a) UV-Visible spectra for known concentration of ferricyanide and (b) calibration plot for ferricyanide.

Calculation S1:

a. From Fig. S16 and S17,

$$y = 1.4458x$$

$$\text{Slope}(m) = 1.4458$$

Therefore at 7.2 h, Absorbance (y) = 0.07580

Concentration (x) = $0.05242 \times 30\text{mL} = 1.573 \text{ mmol}$

Ferricyanide consumption at 7.2 h = (concentration at 0 hour – concentration at 7.2 h)

$$= (15 - 1.573) \text{ mmol}$$

$$= \mathbf{13.427 \text{ mmol}}$$

b. From Fig. 4e,

$$\text{Faradaic efficiency (\%)} = \frac{\text{ferricyanide charge consumption}}{\text{Theoretical charge passed}}$$

$$= 13.427/13.429$$

$$= \mathbf{99.98 \%}$$

c. From the area under the trace in Fig. 4d,

$$\text{Area} = 4.41088 \text{ V h}$$

$$= 4.41088 \times 3600 = 15879.17 \text{ V s}$$

$$\text{Energy} = \text{Area} \times \text{Current}$$

$$= 15879.17 \times 0.05 \text{ A s V}$$

$$= 793.95 \text{ J}$$

$$\text{Electrical energy output (J/mol}_{\text{Ferricyanide}}) = \frac{793.95}{0.015} \text{ J/mol}_{\text{Ferricyanide}}$$

$$\text{Electrical energy output (kJ/mol}_{\text{Ferricyanide}}) = \mathbf{53 \text{ kJ/mol}_{\text{Ferricyanide}}}$$

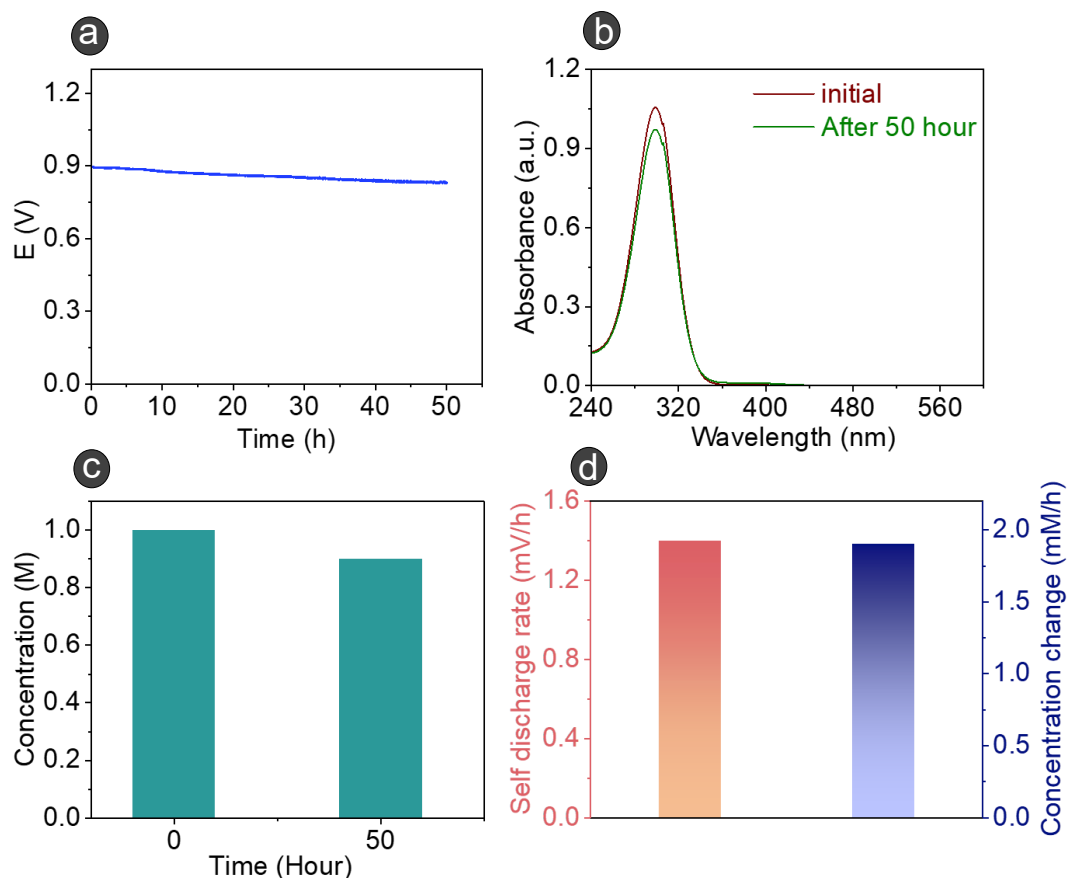


Fig. S18 (a) Self-discharge curve at the open circuit voltage (OCV). (b) UV-Visible spectra of the anolyte (Ar purged solution) before and after 50 hours of self-discharge (corresponding to Fig. R4a). (c) Consumption of anolyte during the self-discharge for 50 hours. (d) Self discharge rate and rate of change in concentration of ascorbic acid in the fuel cell mode.

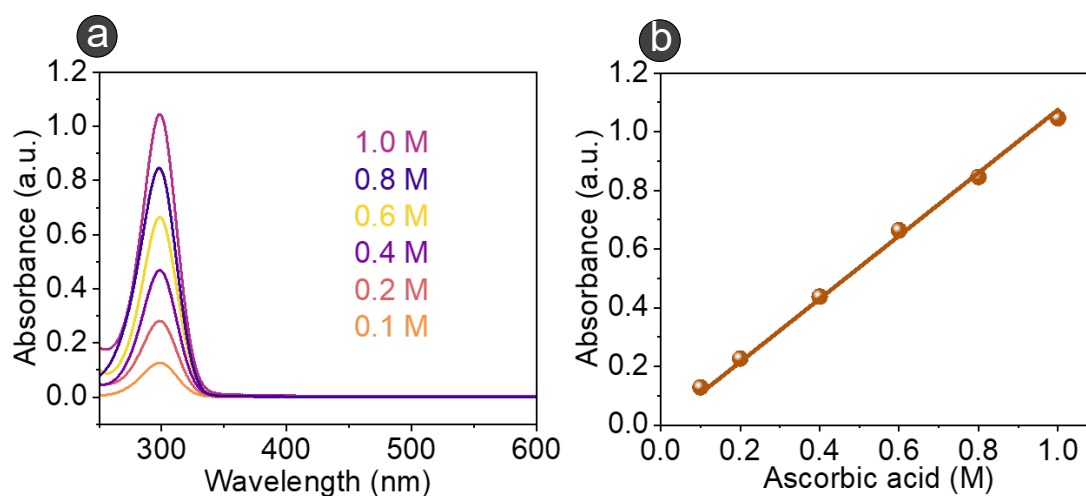


Fig. S19 (a) Calibration plots for ascorbic acid using UV-Vis absorption spectra. (b) Linear fit between absorbance at 300 nm and concentration of ascorbic acid.

Calculation S2:

From Fig. S18 and S19,

$$y = 1.0755x$$

$$\text{Slope}(m) = 1.0755$$

$$\text{Therefore at 50 h, Absorbance } (y) = 0.97314$$

$$\text{Concentration } (x) = 0.97314/1.0755 = 0.90482 \text{ M}$$

$$\text{Change in concentration} = (\text{Initial concentration} - \text{final concentration})$$

$$= (1 - 0.90482) \text{ M}$$

$$= \mathbf{0.095 \text{ M}}$$

$$\text{Change in concentration per hour} = 0.095 / 50 = 0.0019 \text{ M/h} = \mathbf{1.9 \text{ mM/h}}$$

From Fig. S18,

$$\text{Self-discharge rate} = E_{\text{initial}} - E_{\text{final}}/\text{time}$$

$$= 0.9 - 0.83/50$$

$$= 1.4 \text{ mV/h}$$

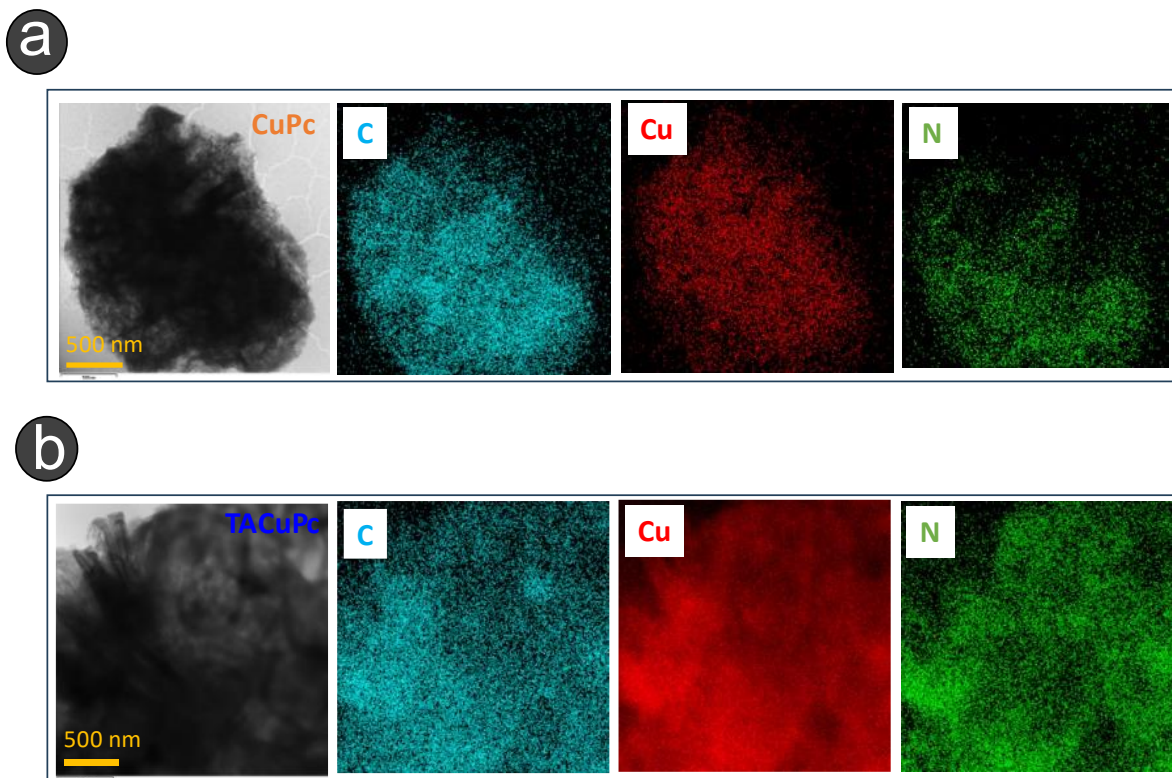


Fig. S20 Scanning electron microscopy images and corresponding elemental mappings for C, Cu and N for (a) CuPc and (b) TACuPc composite electrodes.

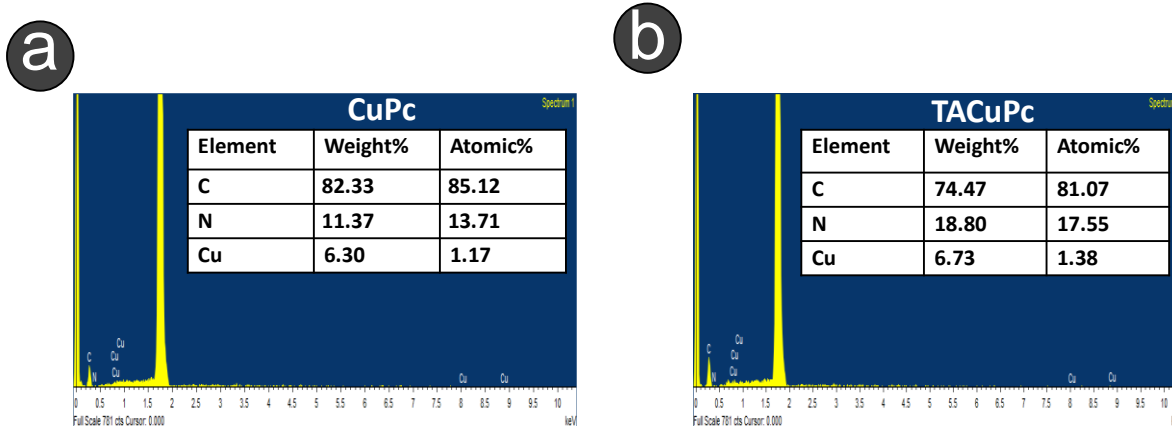


Fig. S21 EDX spectra and elemental analysis table for (a) CuPc and (b) TACuPc composite electrodes.

References:

- 1 E. A. Lukyanets and V. N. Nemykin, *J. Porphyr. Phthalocyanines*, 2010, **14**, 1–40.
- 2 M. H. Haider, H. S. Al-Lami and A. A. Al-Fregi, *Baghdad Sci. J.*, 2016, **13**, 0221.
- 3 F. Fasiulla, *Orient. J. Chem.*, 2022, **38**, 1124–1130.
- 4 J. Alzeer, P. J. C. Roth and N. W. Luedtke, *Chem. Commun.*, 2009, 1970–1971.
- 5 J. Yang, J. Tao, T. Isomura, H. Yanagi, I. Moriguchi and N. Nakashima, *Carbon N. Y.*, 2019, **145**, 565–571.
- 6 H. Genc Bilgicli, A. T. Bilgiçli, T. Alagöz, A. Günsel, M. Zengin and M. N. Yarasir, *Appl. Organomet. Chem.*, 2023, **37**, e7243.